2023 IEEE Symposium on Electromagnetic Compatibility & Signal/Power Integrity (EMC+SIPI) | 979-8-3503-0976-8/23/$31.00 ©2023 IEEE | DOI: 10.1109/EMCSIPI50001.2023.10241522

Characterization and Modeling of Sparkless Discharge to a Touch Screen Display

Jianchi Zhou, Cheung-Wei Lam
Apple Inc.
Cupertino, USA
jianchi_zhou@apple.com, lam@apple.com

Zhekun Peng, Daryl Beetner,
EMC Laboratory
Missouri University of Science and Technology
Rolla, MO, USA
pengzhe@mst.edu, daryl@mst.edu

David Pommerenke
Institute of Electronics
Graz University of Technology
& SAL Graz EMC lab
Graz, Austria
david.pommerenke@tugraz.at

***Abstract*—Although corona discharge to a touchscreen display is not associated with the spark, it could cause soft and hard failures due to electromagnetic coupling to sensitive electronics beneath the glass. Experimental data were obtained to characterize these sparkless discharges and an equivalent circuit model was constructed to predict the resulting coupling to touchscreen electronics. Measurements and simulation indicate that a thinner glass and a higher touchscreen indium-tin-oxide (ITO) sense trace impedance both lead to higher ESD risk by delivering higher energy into the sensing IC. A CST co-simulation model is proposed and is shown to model the displacement current accurately. Charge movement and dissipation on the glass surface is represented using a disk with conductivity proportional to the reciprocal of radial distance. Dust figure measurements were used to study the effects of the glass type, glass thickness and voltage level on the corona discharge and the current coupled to the touchscreen patch on the display. These results can be used to drive full wave co-simulation models which try to anticipate the impact of sparkless discharges on the touchscreen electronics.**

Keywords—ESD; corona discharge; modeling; touchscreen; mobile electronics

I. Introduction

Corona discharge leads to potential risk for soft and hard failures when discharging to the display surface of a mobile device. Although the glass provides insulation from direct sparking to the internal electronics, problems may occur due to electromagnetic coupling [1-3]. Capacitive coupling to the sensing pixel, for example, can cause burnout of the ITO (Indium tin oxide) trace which feeds the sense circuitry.

Characterization of the corona discharge to a display has been presented in [4-6] to evaluate the energy level of such an event. A substitution board system was developed to measure the displacement current coupled to the sense electronics in a controlled environment. A simulation methodology using a current source reconstructed using a genetic algorithm was proposed for circuit and full wave simulation of the sparkless discharge event [5]. The current source, however, can only be implemented for a test case in which the current has already been measured. A simulation method that is applicable to a general device under test is needed when the measurement data are not available.

Although the circuit model in [5] can provide estimates for the ITO trace current, the accuracy of the simulated current is limited because it is based on a simplified RC representation of the display geometry. To improve the accuracy of the estimated current, a Computer Simulation Technology (CST) co-simulation approach was proposed which included the full details of the test structure. The excitation source used in the previous study [5] were reconstructed based on the measurement data using both circuit simulation and the CST co-simulation approach. Although those models have been verified to generate estimated trace currents with a good correlation with the measurement data, this simulation can only be used as verification after the ITO trace current has been measured. For a product at the early design stage, this measurement data may not be available.

The difficulty of modeling the corona discharge is applying the excitation source to the nonconductive glass surface. To develop an accurate model that represents the charge deposition on the glass surface and can be used in a CST co-simulation model, the charge deposited on the glass surface can be visualized experimentally using the Lichtenberg's dust figure method [4, 7]. This approach has been previously used to observe the branching charge structure resulting from a corona discharge to a display [4]. The radially decreasing charge density from the discharge point indicates decreasing conductivity on the ionized air along the surface with distance during the corona discharge. The effects of the voltage level and humidity for two different types of glass on the diameter were studied [4]. The initial results indicate that a higher humidity leads to a smaller diameter dust figure and a higher voltage leads to a larger diameter. This study does not, however, reveal the effects of the glass thickness and other touchscreen design parameters on the dust figure characteristics.

Improved simulation models of corona discharge based on the previous work will be developed in this paper and will be verified using measurements on a substitution board representing a touchscreen display. The main advantage of the developed simulation models is that they allow use of a voltage source that is less dependent on system parameters than the reconstructed current used in previous models that was based on measurements of the ITO trace current. A measurement system is also built which allows controlled measurements of the dust figures generated during a corona discharge and the current coupled to a capacitive touchscreen pixel. This system was used to study for the effects of glass type, glass thickness and the discharge voltage on the dust figure and coupled current. These results provide a simulation reference for modeling the charge propagation on the glass surface. The simulation models are presented in Section II. Measurements are presented in Section III, and conclusions are presented in Section IV.

II. Simulation Methodology

A. Current Measurement Setup

In [6], the displacement current coupled to touchscreen electronics during a sparkless discharge were measured using the substitution board shown in Fig. 1. The effects of the glass thickness, nearby ground planes, and the resistance of the ITO trace were studied using statistical analysis. Fig. 2 shows the path of current from the discharge point into the sensing IC. Due to the variation of IC behaviors, the model excludes the sensing IC and focuses on other factors. The critical parameters for the equivalent model are Csp, the capacitance from the glass to the trace, Cpg, the capacitance from the trace to the ground plane, and R_{ITO}, the resistance of the trace. Csp is determined by the pixel size and the glass properties. Cpg is determined by the design of the grounding structures inside the device. R_{ITO} is determined by the ITO layout within the touch screen. This resistance was varied in the substitution board by placing metal electrode leadless face (MELF) resistors with different values on the board. For the substitution board used here, the capacitances were extracted using CST E-static simulation [8] and were used in the circuit simulation presented next.

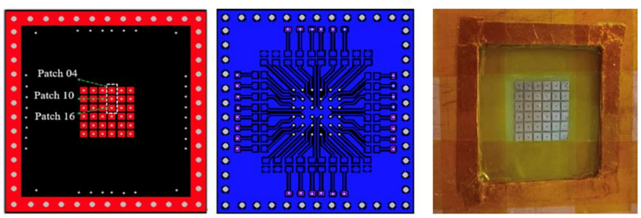

(a) (b) (c)

Fig. 1. Substitution board for measuring the displacement current. (a) Top layer; (b) Bottom layer; (c) The glass pressed against the top layer. The resistors are soldered to traces connected to a coaxial cable connected to an oscilloscope.

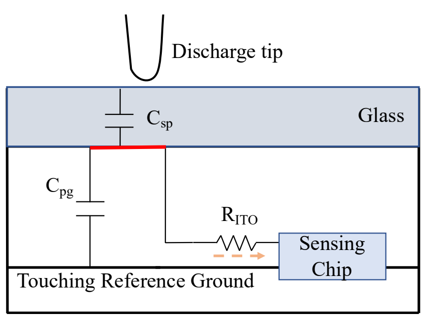

Fig. 2. An equivalent model for the display. Csp represents the capacitance between the charged display surface and the touch pixel. Cpg represents the capacitance between the touch pixel and the ground plane. R_{ITO} represents the impedance of the ITO trace to the sensing chip.

B. Circuit Modeling

The application of the simulation methodology proposed in [5] is limited since it uses an excitation source based on measured data, and this source is not valid if any significant changes are made to the system. An alternative method is to use the voltage source from an ESD generator as the excitation source. Although the ESD gun air discharge tip may not be fully discharged during a corona discharge, a simulation model which assumes the charge has been fully transferred is still valid for comparative simulations which evaluate the impact of design-related changes to the capacitor and resistor values shown in Fig. 2 and to estimate the worst case current flowing into the IC.

A circuit model using an ESD gun contact discharge model as an excitation source is shown in Fig. 3. This model is used to drive the RC equivalent circuit in Fig. 2. An ideal connection between the injection port and the RC circuit indicates this is a worst-case assumption that essentially treats the glass as a conductive surface.

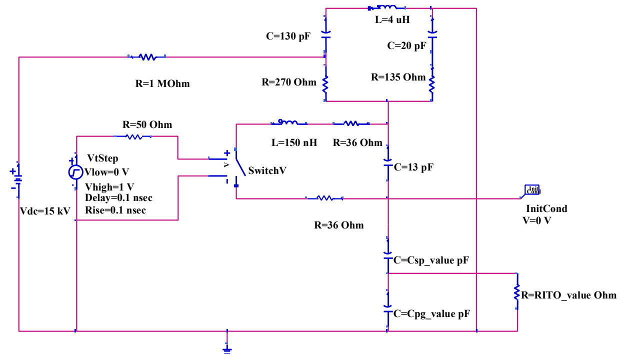

Fig. 3. A circuit model using the ESD gun voltage as the source excitation.

The influence of Csp, Cpg and R_{ITO} were simulated by sweeping the parameters in the circuit simulation. Since thermal damage to the ITO trace is a more severe risk for the device than soft failure, the energy dissipated by the trace during one discharge is analyzed instead of the peak value of the transient current. Plots of the energy delivered to the trace are presented in Fig. 4 as a function of changes in Csp, Cpg and R_{ITO}. When R_{ITO} is fixed and the capacitance Csp and Cpg are swept, the energy increases as Cpg decreases and Csp increases. Similarly if Csp is fixed and Cpg and R_{ITO} are swept, the energy increases as R_{ITO} increases in the sweep range. This trend indicates that the thinner the glass, the poorer the grounding of the display, and the higher the ITO impedance (≤15 kohm), the higher the risk of thermal damage. To improve the ESD robustness of the display, the designer should provide a solid grounding structure which maximizes Cpg and should reduce the ITO trace impedance.

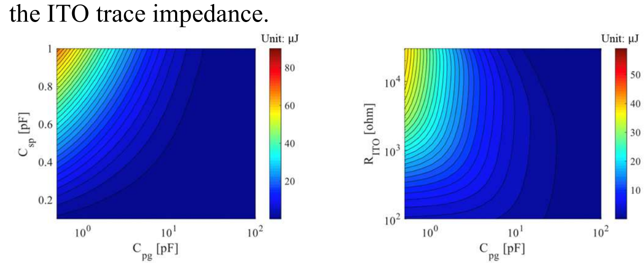

Energy colormap, fixed R_{ITO}=10kohm and sweep C_{sp}, C_{pg} Energy colormap, fixed C_{sp}=650fF and sweep C_{pg}, R_{ITO}

Fig. 4. Simulated energy into the ITO trace while sweeping Csp, Cpg and R_{ITO}.

C. Full-wave Co-simulation

A full-wave model of the substitution board was combined with the ESD gun circuit model to obtain an accurate estimate of the ITO trace current as shown in Fig. 5. A conductive disk was used to represent the charge propagation of the corona discharge across the glass surface. The radius of the disk can be determined from dust figure measurements, as will be discussed in Section III. The conductivity of the disk is also tuned based on measured current waveforms.

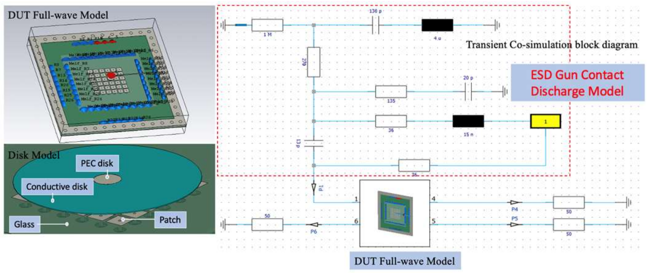

Fig. 5. CST Co-simulation model for the test board. Upper left: full-wave model of the substitution board. Lower left: conductive disk representing charge flow on the glass surface. Right: circuit model representing ITO trace and other components connected to the sense patch on the display.

A Perfect Electrical Conductor (PEC) disk was initially used in the simulation. Two different sizes of disk were used, one that covers the center patch only and one that covers the center and the first adjacent patches. The current delivered to the center patch is compared to measurements since the center patch has the highest current among all the patches. An example of the waveforms is shown in Fig. 6 when the disk covers only the center patch in the co-simulation.

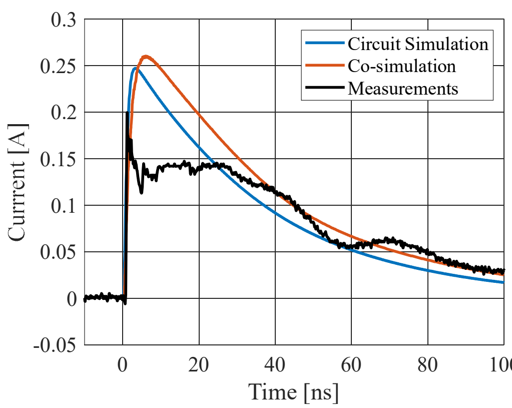

Fig. 6. Comparison of the measured and simulated current waveform seen at the center patch.

An improved model was developed by assigning the disk conductivity to be proportional to reciprocal function in the radial direction to account for charge dissipation across the glass surface, as shown in Fig. 7. The varying conductivity was achieved using the CST macros tool "create spatially varying material from analytical formula" [9]. The radius of the disk was obtained from dust figure measurements. A small PEC disk is placed in the center of the disc to avoid a singularity at the discharge point. The conductivity of the disk is given by:

$$\boldsymbol{Conductivity} = \mathbf{3} \cdot \boldsymbol{r}^{-\mathbf{1}} \quad (1)$$

where the r is the radius in cylindrical coordinates and the constant 3 was estimated from measured data regarding the peak current. The measured and simulated current delivered to the patch are shown in Fig. 8. The energy and rise time associated with the simulated current waveform is compared with the measurements in Table 1. It's a reasonable prediction because it's limited by the lack of real-time ionization process.

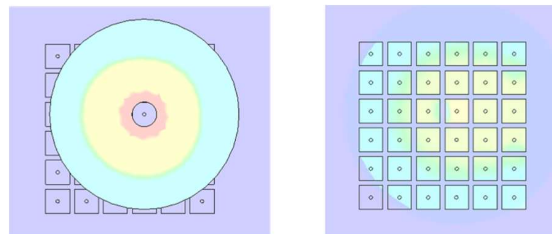

Fig. 7. Surface current distribution on the disk and the patches.

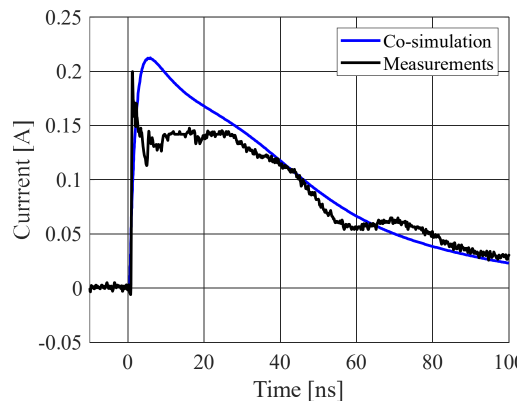

Fig. 8. Measured and simulated current delivered to the center patch during a corona discharge, when using a circular disk with conductivity proportional to the reciprocal of radial distance in the co-simulation.

TABLE I. ENERGY AND RISE-TIME OF CURRENT DELIVERED TO CENTER PATCH ITO TRACE

	Energy [uJ]	***Rise time [ns]***
Measurement	9.83	0.5
Co-simulation	14.38	2.28

III. DUST FIGURE MEASUREMENTS

A. Measurement Setup

To develop an accurate model of the charge deposition on the glass surface for the CST co-simulation, the charge deposited on the glass surface can be visualized using dust figure measurements. To make the dust figure measurements, the glass is cleaned and dried before a discharge is made, and then a fine dust like printer toner is blown on the surface just after the discharge is made. The dust is attracted to the deposited charge and shows a branching structure indicating the charge density on the glass surface.

An ESD generator with a 330 pF charge capacitance can create multiple discharges to an insulating surface [6]. These multiple discharges can distort dust figure measurements, since the dust figure from the first discharge can be obscured by the second discharge, even if the first discharge was of higher magnitude. A test fixture was created as shown in Fig. 9 where the corona discharge to a glass surface could be measured in a highly repeatable fashion and where the capacitance of the discharge structure was lower than 330 pF to eliminate the multiple discharge events. The test fixture was created by attaching a metal rod to the end of an insulating bar and connecting the insulating bar to a ground plane with a hinge. The insulating bar and hinge allows the rod to fall in a controlled manner. The rod is charged when it is in the raised position, and is then allowed to fall onto a glass surface where it creates a corona discharge. A series of capacitors with an equivalent capacitance of 20 pF were connected between the air discharge tip and ground to provide additional charge at the tip, albeit less than the ESD generator. A high-voltage source was connected to a spherical ball that comes into contact with the metal rod when it is in the raised position. The discharge current was measured during the corona discharge using a Fischer F-65 current probe. Dust figures were obtained after each discharge event.

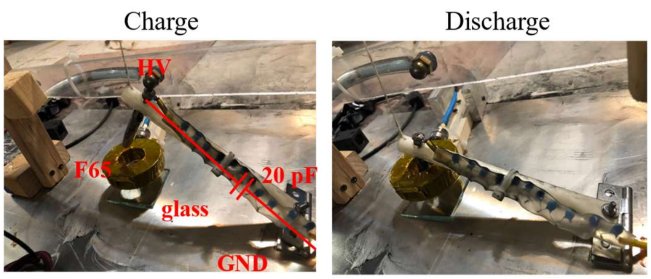

Fig. 9. Dust figure measurement setup.

The discharge current and dust figures generated by a discharge to three types of glass commonly used in mobile displays (HIE Gorilla glass, borosilicate, and sodalime) were tested using this setup. The impact of the voltage level applied to the charged rod and of the glass thickness on the dust figure and the discharge current was investigated. Charge voltages ranged from 9 kV to 15 kV and glass thickness ranged from 0.55 mm to 4 mm.

B. *Influence of Glass Type*

The dust figures shown in Fig. 10 were obtained for three different types of glass. Each glass sheet was 2 mm thick and the metal rod was charged to 15 kV. Although the branching patterns of the dust figures are not identical, the dust figure diameters are in the same range, from 3.8 to 4.8 cm. Measurements over a large dataset show only a weak correlation between the glass material and the size and shape of the dust figure. The current and transferred charge, however, is related to the material because the capacitance from the surface to the ground plane depends on the permittivity of the material. As shown earlier a higher Csp leads to a higher current and energy at the ITO trace. The measurements confirm this relationship, and show that the highest current is associated with the highest permittivity glass as the current in HIE (relative permittivity ε_r=8.1) was generally greater than in sodalime (ε_r=6.4) which was generally greater than in borosilicate (ε_r=4.5), as will be shown in detail in Sub-Section E.

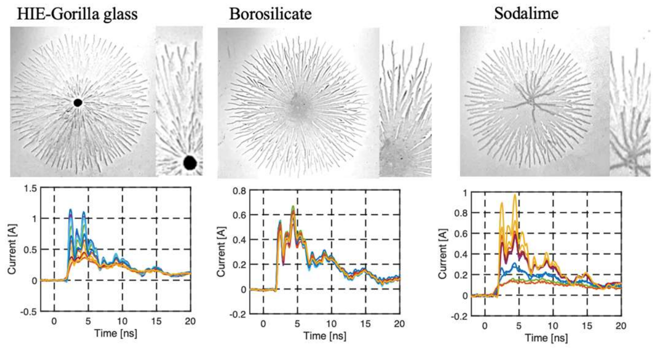

Fig. 10. Dust figures and discharge currents for different types of glass. Each glass sheet was 2 mm thick. The ESD gun was charged to 15 kV.

C. *Influence of Voltage Level*

The discharge current and the dust figure diameter increase with the charge voltage of the metal rod, as shown in Fig. 11 for discharges to 2 mm thick borosilicate glass. The dust figure branching pattern remains the same glass when voltage levels are up to 15 kV. For the three different types of glass, the branching pattern are different as shown in Fig. 10, but the same increasing trend in diameter with charge voltage was observed.

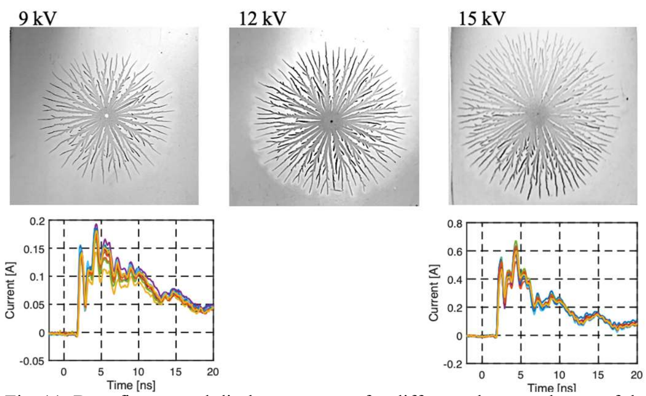

Fig. 11. Dust figures and discharge current for different charge voltages of the metal rod, when discharging to 2 mm thick borosilicate glass.

D. *Influence of Glass Thickness*

When the glass thickness increases, the capacitance between the charged surface and the ITO trace decreases. As a result, a lower current is expected for thicker glass. It is incorrect, however, to assume that the diameter of the dust figure should also decrease since the current is lower. As the thickness increases, the coupling to the ground plane becomes weaker and the charge stays on the surface and travels further before dissipating. An example is shown in Fig. 12 for a measurement of a 15 kV corona discharge to the borosilicate glass. The current was reduced from 1.4 A to 0.3 A when the glass thickness was increased from 0.7 mm to 3.8 mm, while the diameter of the dust figure increased from 2.5 cm to 5.0 cm.

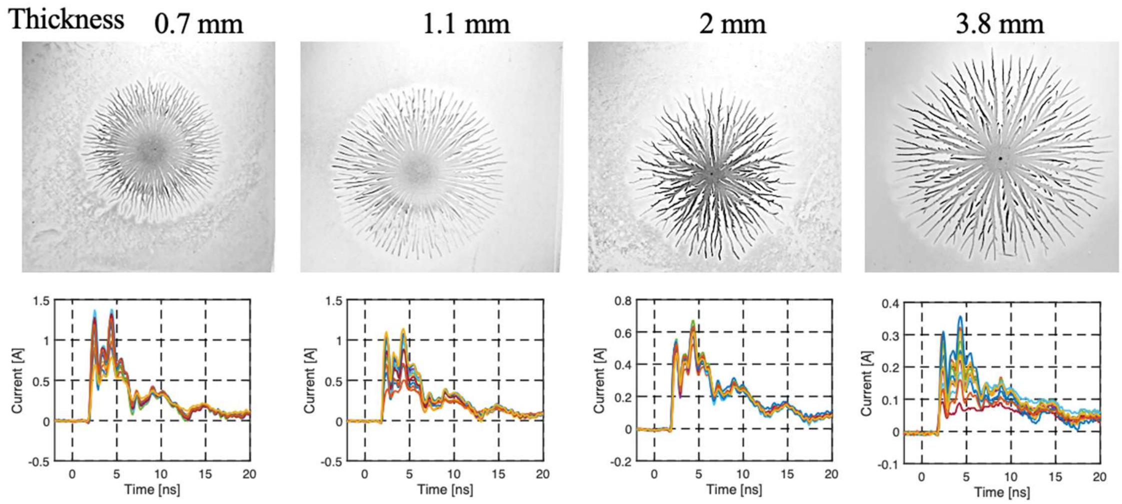

Fig. 12. Dust figure and the discharge current for different thicknesses of borosilicate during a 15 kV corona discharge.

E. *Data Analysis*

The impact of the glass type, glass thickness, and discharge voltage on the dust figure diameter, the discharge current and the charge delivered to the sensor IC are summarized in Fig. 13 and Fig. 14 using the average value of five repeated measurements for each test setup. The type of glass only weakly impacts the dust figure diameter. The level of current delivered to the sensor IC increases with the permittivity of the glass. The higher the permittivity, the higher the capacitance Csp, which leads to a higher current.

The dust figure diameter and the current increases with the charge voltage for all three materials. When the glass thickness increased, the dust figure diameter increases but the current reduces. The diameter of the conductive disk used in co-simulation should be changed with the charge voltage and the glass thickness, though the diameter does not need to be changed with glass type. The results in Fig. 13 and Fig. 14 can be used by the designer to determine the disk size. The equation for conductivity, however, should still be tuned based on measurements.

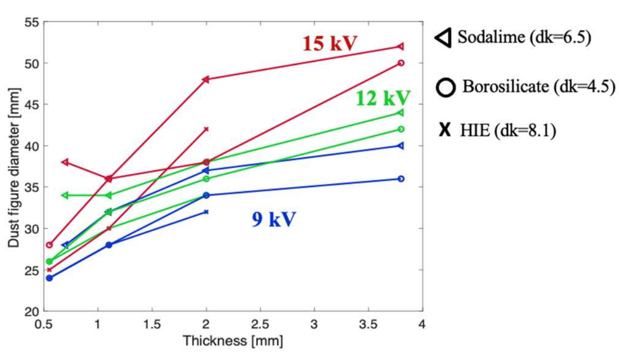

Fig. 13. Dust figure diameter as a function of glass thickness, for different types of glass (different dielectric constant) and different discharge voltage levels.

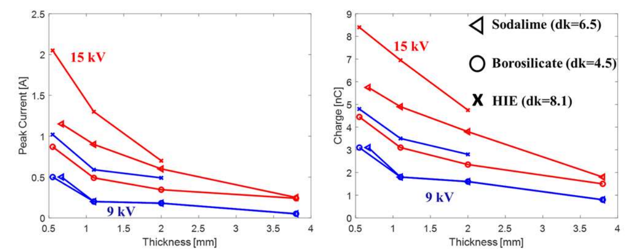

Fig. 14. Peak current and charge transferred to the sensor IC as a function of the glass thickness, for different types of glass and different discharge voltage levels.

The data were analyzed using the average measurement in Fig. 13 and Fig. 14 because the results varied from one discharge to another. Fig. 15 shows the variation in the peak current and the transferred charge over the measurements for borosilicate glass when the glass thickness ranged from 0.55 mm to 4 mm and the discharge level ranged from 9 kV to 15 kV. The trend in the peak current and transferred charge with the discharge voltage level and the glass thickness still hold when accounting for the variations in results.

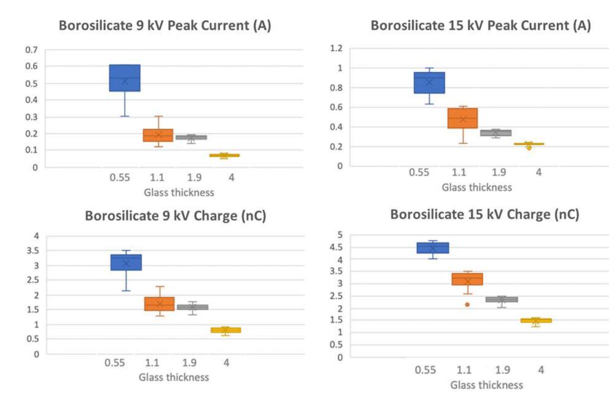

Fig. 15. Peak current and transferred charge for borosilicate glass.

IV. Conclusions

The corona discharge to a touchscreen display has been characterized through simulations and measurements on a substitution board representing the display. A simulation methodology using an equivalent circuit for the touchscreen and using an ESD gun voltage source as an excitation was also proposed and verified through measurements. While this simulation model overestimates the current delivered to the touchscreen electronics, it can provide useful early guidance toward the touchscreen display design before the actual product is ready for testing.

Simulations and measurements show that thinner glass and higher ITO trace impedance lead to a higher ESD risk since more energy is delivered to the ITO trace. As increasing the glass thickness may not be a realistic option, one can improve the ESD robustness by providing a better grounding for the touch pixels which will increase the Cpg capacitance between the pixel and ground and provide an alternate return path for the current rather than flowing through the ITO.

To improve the accuracy of simulations, a full-wave model was proposed where a conductive disk was used to model the charge propagation on the glass surface. Conductivity proportional to the reciprocal of radial distance was assigned to the disk to account for charge dissipation across the glass surface. The disk size can be determined based on dust figure measurement from the dust figure diameter. Initial results using this method shows a good correlation between the observed current and those found in measurements. This model is capable of predicting the energy delivered to the ITO trace and the current derivative, which is an indication of the potential to create a soft failure.

To guide the development of the disk model used in full wave simulations, the charge propagation on the glass surface was studied using the Lichtenberg dust figure visualization method. The dust figure study provides a better understanding of the effect of the glass type and thickness and the voltage level on the charge distribution on the glass. The dust figure diameter increases as the volage level and the glass thickness increases. The measured dust figure diameter could be used as reference for the conductive disk in the simulation. In this study, the conductivity of the disk was varied as $3*r^{-1}$, where r is the radius of the disk. The value of the constant used in this relationship should be tuned using measurements for the conditions that are being simulated. Predicting the value of the conductivity constant based on the characteristics of the glass and discharge parameters is a topic for future study.

Acknowledgments

This work was supported in part by the National Science Foundation (NSF) under Grant IIP-1916535.

References

[1] J. Ko, K. Kim, and H. Kim, “System-level ESD immunity of mobile display driver IC to hard and soft failure,” Elect. Electron. Eng., vol. 13, no. 1, pp. 329–335, 2012.

[2] K. Kim and Y. Kim, “Systematic analysis methodology for mobile phone’s electrostatic discharge soft failure,” IEEE Trans. Electromagn. Compat., vol. 53, no. 3, pp. 611–618, Aug. 2011.

[3] Z. Li, P. Maheshwari, and D. Pommerenke, “Measurement methodology for field-coupled soft errors induced by electrostatic discharge.

[4] Y. Gan *et al*., "Experimental Characterization and Modeling of Surface Discharging for an Electrostatic Discharge (ESD) to an LCD Display," in *IEEE Transactions on Electromagnetic Compatibility*, vol. 60, no. 1, pp. 96-106, Feb. 2018

[5] H. Rezaei *et al*., "Experimental characterization and methodology for full-wave modeling of ESD to displays," *2020 IEEE International Symposium on Electromagnetic Compatibility & Signal/Power Integrity (EMCSI)*, 2020, pp. 182-187.

[6] Z. Peng *et al*., "Trend Analysis of Dissipated Electrostatic Discharge Energy in Touchscreen Displays," *2020 IEEE International Symposium on Electromagnetic Compatibility & Signal/Power Integrity (EMCSI)*, 2020, pp. 188-193.

[7] J. Zhou *et al*., "IEC 61000-4-2 ESD test in display down configurationfor cell phones," *2016 IEEE International Symposium on Electromagnetic Compatibility (EMC)*, 2016, pp. 713-718.

[8] CST Studio Suite help, “Electrostatic Solver Overview.” [Online]. Available:https://space.mit.edu/RADIO/CST_online/mergedProjects/3D/special_overview/special_overview_electrostatic_solver_overview.htm

[9] CST Studio Suite help, “Material Objects.” [Online]. Available: https://space.mit.edu/RADIO/CST_online/cst_studio_suite_help.htm